ELSEVIER

Contents lists available at ScienceDirect

Protein Expression and Purification

journal homepage: www.elsevier.com/locate/yprep



Research Article

CUREs for high-level Galectin-3 expression

Alexander A. Charbonneau, Elizabeth J. Reicks, John F. Cambria, Jacob Inman, Daria Danley, Emmie A. Shockley, Ravenor Davion, Isabella Salgado, Erienne G. Norton¹, Lucy J. Corbett, Lucy E. Hanacek, Jordan G. Jensen, Marguerite A. Kibodeaux, Tess K. Kirkpatrick, Keilen M. Rausch, Samantha R. Roth, Bernadette West, Kenai E. Wilson, C. Martin Lawrence, Mary J. Cloninger*

Department of Chemistry and Biochemistry, Montana State University, Bozeman, MT, 59717, USA

ARTICLE INFO

Keywords: Galectins Galectin-3 Carbohydrate recognition domain Autoinduction Protein expression Lac repressor Time-dependent fluorescence

ABSTRACT

Galectins are a large and diverse protein family defined by the presence of a carbohydrate recognition domain (CRD) that binds β -galactosides. They play important roles in early development, tissue regeneration, immune homeostasis, pathogen recognition, and cancer. In many cases, studies that examine galectin biology and the effect of manipulating galectins are aided by, or require the ability to express and purify, specific members of the galectin family. In many cases, *E. coli* is employed as a heterologous expression system, and galectin expression is induced with isopropyl β -galactoside (IPTG). Here, we show that galectin-3 recognizes IPTG with micromolar affinity and that as IPTG induces expression, newly synthesized galectin can bind and sequester cytosolic IPTG, potentially repressing further expression. To circumvent this putative inhibitory feedback loop, we utilized an autoinduction protocol that lacks IPTG, leading to significantly increased yields of galectin-3. Much of this work was done within the context of a course-based undergraduate research experience, indicating the ease and reproducibility of the resulting expression and purification protocols.

1. Introduction

Galectins are beta-galactoside binding proteins that play important roles in many intercellular recognition processes including those involved in early development, tissue regeneration, immune homeostasis, pathogen recognition, and cancer progression [1–4]. Sixteen galectins, all including a conserved carbohydrate recognition domain (CRD), have been sorted into three galectin subfamilies [5]. Prototype galectins exhibit two CRDs that assemble into noncovalent homodimers in solution (depicted in Fig. 1A), whereas tandem-repeat galectins consist of an N-terminal CRD, an unstructured linker, and a C-terminal CRD (illustrated in Fig. 1B). Galectin-3, in contrast, is the sole member of the chimera galectin subgroup that features a disordered N-terminal domain (NTD) and a C-terminal CRD (as shown in Fig. 1C).

Galectin-3 is reported to aggregate via interactions of its NTD [6], but the need for both dimeric galectins (prototype and tandem-repeat) and a variably oligomeric galectin (chimera) is currently unclear.

Histological mapping of the galectins indicates they are broadly distributed in the mammalian body and are co-expressed in many tissues and organs [7], which raises the question of whether galectins from different subfamilies act cooperatively. Indeed, when galectin-1, galectin-3, and galectin-7 were studied as mixtures for *in vitro* cell-based assays, synergistic results were observed [8]. These reports provide a strong impetus for additional studies using galectins from all three subfamilies, but such studies are currently hindered by insufficient quantities of galectin-3.

All galectins have a conserved eight-amino acid sequence motif in their carbohydrate-binding pocket [3]. Known native carbohydrate ligands for the galectins have recently been reviewed [4], and although some differences in carbohydrate selectivity have been reported, all galectins bind to beta-galactosides such as lactose [9,10]. Galectins all have weak monovalent carbohydrate binding interactions, relying on multivalent interactions to increase the specificity and selectivity of their protein/carbohydrate interactions [5,11–13]. Small molecule

 $^{^{\}ast}$ Corresponding author.

E-mail address: mcloninger@montana.edu (M.J. Cloninger).

¹ Current Affiliations: 1) St. Jude Graduate School of Biomedical Sciences, St. Jude Children's Research Hospital, Memphis, TN 38105, USA, and 2) Department of Immunology, St. Jude Children's Research Hospital, Memphis, TN 38105, USA.

inhibitors of galectins have been developed, including thiodigalactosides with aryl groups at the C₃–OH position [14,15]. The derivatized thiodigalactosides represent an extension of earlier work to develop thiogalactoside derivatives with good galectin-binding activity [16,17].

Many reports describe the expression of recombinant human galectins in $E.\ coli\ [18–21]$. One common and effective method for the purification of these galectins is passage over a lactose affinity column [21, 22]. However, in this case, extensive dialysis to remove lactose is then required. Insertion of a histidine tag allows for purification using immobilized metal affinity chromatography, and we have found that the presence of the His $_6$ -tag does not change protein activity in binding and aggregation assays [13,23].

Here, we report enhanced expression and purification of His-tagged galectin-3, both for the full-length protein and the carbohydrate recognition domain. Notably, IPTG is frequently used to induce expression in *E. coli*. However, as shown here, galectin-3 binds IPTG with micromolar affinity, potentially resulting in feedback inhibition of galectin expression and reduced yields. Here, we employ the Studier autoinduction protocol [24] to circumvent this inhibitory feedback loop and demonstrate significantly increased yields for the galectin-3 CRD (Gal-3 CRD) as well as the full-length protein. Most of this work was performed by students participating in a course-based undergraduate research experience (CURE), which demonstrates the successful implementation of the described procedures by novice researchers. In other words, the "CURE" contributed significantly to a "cure" for high-level expression of galectin-3.

2. Materials and methods

2.1. Galectin-3 expression clones

The expression vector for the full-length human His $_6$ -tagged galectin-3 construct (pEXP14-6xHis-Gal-3) was described previously [23]. The galectin-3 carbohydrate recognition domain (Gal-3 CRD, amino acids 112–250) was cloned as previously described [25,26]. Briefly, fragments of the *Homo sapiens* galectin-3 gene (NM_002306.4) were amplified using polymerase chain reactions (PCR) with the pGEX-6p-Gal-3 vector as a template. The sequences of the forward and reverse primers are given in Supplementary Table S1. The cloning strategy introduced attB sites, a Shine-Dalgarno sequence, and a minimal N-terminal 6x-His-tag. The amplified products were inserted into pDONR201 (Invitrogen) by site-specific recombination using the Gateway BP clonase reaction following the manufacturer's instructions. Sequence-verified constructs were then transferred into pDEST14 (Invitrogen), again using Gateway site-directed recombination, yielding expression vectors pEXP14-6 \times His-Gal-3_CRD.

2.2. IPTG induction

For galectin-3 and Gal-3 CRD expression, BL21(DE3)-pRIL *E. coli* (Stratagene) were transformed with pEXP14-6 \times His-Gal-3 and pEXP14-6 \times His-Gal-3_CRD, respectively. A single colony was used to inoculate 5 mL of LB media (10 g tryptone, 5 g NaCl, and 5 g yeast extract per L) with 100 $\mu g/mL$ ampicillin and 34 $\mu g/mL$ chloramphenicol and grown at 37 °C with shaking at 250 rpm for 16 h. Then, 750 mL LB media [27] in a 2.8 L baffled Fernbach flask containing 100 $\mu g/mL$ ampicillin and 34 $\mu g/mL$ chloramphenicol was inoculated with 750 μL of the starter culture and grown at 37 °C with shaking at 250 rpm until OD_600 reached 1.0. IPTG was then added to the indicated final concentration (0 mM, 0.1 mM, 0.5 mM, 1 mM, 2 mM, or 5 mM), and cultures were incubated at 37 °C with shaking at 250 rpm for 4 h. Cells were harvested by centrifugation at 5000×g for 20 min, supernatant was discarded, and the pellets were stored at -80 °C.

2.3. Autoinduction

For autoinduction of full-length galectin-3 and Gal-3 CRD, BL21 (DE3)-pRIL *E. coli* (Stratagene) were transformed with pEXP14-6 \times His-Gal-3_CRD or pEXP14-6xHis-Gal-3 as needed. A single colony was then used to inoculate 5 mL of LB media with 100 µg/mL ampicillin and 34 µg/mL chloramphenicol and grown at 37 °C with shaking at 250 rpm for 4 h. Then, 750 mL ZYP-5052 autoinduction media ([24], see below) in a baffled 2.8 L Fernbach flask containing 100 µg/mL ampicillin and 34 µg/mL chloramphenicol was inoculated with 750 µL of the starter culture and grown at 37 °C with shaking at 250 rpm for 18 h. Cells were harvested by centrifugation at 5000×g for 20 min, supernatant was discarded, and the pellets were stored at $-80\ ^{\circ}\text{C}.$

2.4. ZYP-5052 autoinduction media

We utilized the autoinduction protocol of Studier [24]. Specifically, 1 L of autoinduction media was composed of 10 g tryptone, 5 g yeast extract, 930 mL $_{12}$ 0, 1 mL 1 M MgSO₄, 100 $_{12}$ L 10,000x trace metal stock solution, and 50 mL 20x NPS. After autoclaving, 20 mL of filter-sterilized 50 x 5052 sugar stock solution was added.

The 10,000x trace metal stock solution was composed of 25 mL 0.1 M FeCl $_3$ in 0.1 M HCl, 0.111 g CaCl $_2$, 0.099 g MnCl $_2$ ·4H $_2$ O, 0.144 g ZnSO $_4$ ·7H $_2$ O, 0.024 g CoCl $_2$ ·6H $_2$ O, 0.017 g CuCl $_2$ ·2H $_2$ O, 0.024 g NiCl $_2$ ·6H $_2$ O, 0.026 g Na $_2$ SeO $_3$ ·5H $_2$ O, 0.006 g H $_3$ BO $_4$, dissolved in H $_2$ O to a final volume of 50 mL. The 20x NPS stock solution was composed of 33 g (NH $_4$) $_2$ SO $_4$, 68 g KH $_2$ PO $_4$, Na $_2$ HPO $_4$, and dissolved in H $_2$ O to a final volume of 500 mL. The 50x 5052 sugar stock solution was composed of 125 g glycerol, 12.5 g glucose, and 50 g alphalactose, dissolved in H $_2$ O to a final volume of 500 mL, and sterilized by

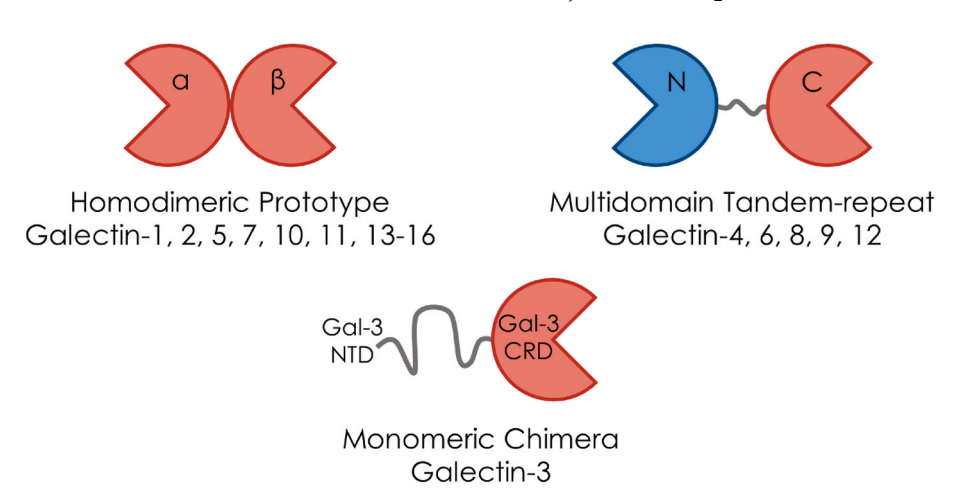


Fig. 1. A schematic representation of the A) prototype, B) tandem-repeat, and C) chimera galectins.

passage through a 0.2 µm filter.

2.5. Purification

Cell pellets were thawed and resuspended at 10 mL/g of cell pellet in lysis buffer (400 mM NaCl, 50 mM Tris-Cl, pH 8). PMSF (0.1 mM) was added to the cell suspension, and cells were lysed by passage through a French press (American Instrument Co., Inc., Silver Springs, MD). The lysate was clarified by centrifugation at 30,000×g for 30 min. The supernatant was then applied to a gravity-flow column containing Ni-NTA agarose (Qiagen). Five flow-through fractions of equal bed volume were collected, and the column was then washed with 10 bed volumes of lysis buffer. Galectins were eluted in 300 mM NaCl, 300 mM imidazole, 50 mM Tris-Cl, pH 8. Protein concentrations were determined by Bradford assay [28] using Protein Assay Reagent (Bio-Rad) and bovine serum albumin as a standard. The purity and mass of each galectin were confirmed by SDS-PAGE. SDS-PAGE gels were imaged with an Invitrogen iBrightTMCL1500 gel imager. Elution fractions containing galectin were then combined. Following the Ni-NTA purification, Gal-3 CRD was dialyzed into PBS. Galectin-3 was subjected to size exclusion chromatography on a calibrated Superdex 75 10/300 GL column (Cytiva, Marlborough, MA, USA) with PBS buffer. Following buffer exchange or dialysis into PBS, galectin concentrations were quantified by OD_{280} , the protein was diluted to 1 mg/mL, and stored at -80 °C in 1 mL aliquots. Extinction coefficients for each construct are given in Supplementary Table S2.

2.6. Analytical size exclusion chromatography

Size exclusion chromatography (SEC), as described above (2.5), was also performed to probe the oligomeric state of each galectin construct. Using PBS, both full-length galectin-3 and Gal-3 CRD showed slower than the expected mobility relative to their monomeric species, signaling an interaction with the matrix (dextran, Supplementary Fig. S1 andS2, respectively). Attempts to disrupt the interaction with increased NaCl concentrations did not resolve this issue.

2.7. Mass spectroscopy

Each of the purified proteins was submitted to the IDEA National Resource for Quantitative Proteomics at the University of Arkansas Medical School to confirm the identities of the purified proteins. The protocol for gel-based MS/MS analysis and the data for characterizations of gal-3 CRD are provided in the Supplementary Data, Fig. S3. Protein probabilities were assigned by the Protein Prophet algorithm [29].

2.8. Fluorescence lifetime binding assays

Fluorescence lifetime binding assays were performed as previously described [23,30]. Lactose or IPTG were titrated across a 96-well quartz micro-plate (Hellma) for the galectin constructs at final concentrations ranging from 1.9 to 6.6 μM in PBS, with three technical replicates for each experiment. Wells were excited at 295 nm and time-resolved emission of individual wells followed at 350 nm using a NovaFluor fluorescence lifetime spectrometer (Fluorescence Innovations) [31,32]. Waveforms were recorded over a total decay time of 128 ns at 2 ps intervals. The fluorescence lifetime data were analyzed as described in the Supplementary Information of Schlick et al. and Bernhard et al. [23,33]. Briefly, the waveforms collected from each lactose/IPTG concentration were fit to a linear combination of the free (Wf) and complexed (Wc) waveforms, yielding the fraction of protein in complex with ligand at each ligand concentration. The data were then fit to the "one-site specific binding" function in GraphPad Prism (Y = $B_{max}{}^{\star}X/(K_D+X);\,Y=$ fraction bound; X = ligand concentration).

2.9. Small scale expression cultures

To assess the influence of a wider range of IPTG concentrations, the protocol for IPTG induction described in section 2.2 was followed with minor modifications. For galectin-3 and Gal-3 CRD expression, BL21 (DE3)-pRIL E. coli (Stratagene) were transformed with pEXP14-6 \times His-Gal-3 and pEXP14-6 × His-Gal-3_CRD, respectively. A single colony was used to inoculate 5 mL of LB media (10 g tryptone, 5 g NaCl, and 5 g yeast extract per L) with 100 $\mu g/mL$ ampicillin and 34 $\mu g/mL$ chloramphenicol and grown at 37 °C with shaking at 250 rpm for 16 h. Then, 500 mL LB media [27] in a 2.8 L baffled Fernbach flask containing 100 $\mu g/mL$ ampicillin and 34 $\mu g/mL$ chloramphenicol was inoculated with $500~\mu L$ of the starter culture and grown at 37 $^{\circ}C$ with shaking at 250 rpm until OD₆₀₀ reached 1.0. The culture was then split between nine 250 mL sterile flasks, and IPTG was added to a final concentration of 0 mM, 0.1 mM, 0.5 mM, 1 mM, 2 mM, 5 mM, 10 mM, 25 mM, or 50 mM, and cultures were incubated at 37 °C with shaking at 250 rpm for 4 h. Cells were harvested by centrifugation at 5000×g for 20 min, supernatant was discarded, and the pellets were stored at -80 °C. Cell pellets were resuspended in 10 mL lysis buffer (400 mM NaCl, 50 mM Tris-Cl, pH 8) supplemented with 0.1 mM PMSF and 1 mM EDTA. Cells were lysed by passage through a French press (American Instrument Co., Inc., Silver Springs, MD). The lysate was clarified by centrifugation at 30,000×g for 30 min. The resulting lysate pellet was resuspended in 10 mL of lysis buffer. For quantification of Gal-3 CRD and full-length galectin-3, $10~\mu L$ of each cleared lysate and resuspended lysate pellet fractions were run on 13 % SDS-PAGE gels alongside a control sample of 2.5 µg purified Gal-3 CRD or full length galectin-3. SDS-PAGE gels were imaged and analyzed with an Invitrogen iBright™CL1500 gel imager. Local-background corrected volumes for each Gal-3 CRD band were normalized to that of the 2.5 μg control band. Cleared lysate and resuspended lysate pellets were quantified for two separate culture growths for each IPTG concentration.

2.10. Statistics

Mean yields and standard deviations for purified Gal-3 CRD were calculated from eluent fractions from at least three replicates for each induction method and IPTG concentration. Replicates consisted of three independently grown cultures from three individual transformant colonies and two individual transformations.

Mean yields and standard deviations for purified full-length galectin-3 were calculated from eluent fractions from four replicates for each induction method and IPTG concentration. Replicates consisted of four independently grown cultures from three individual transformant colonies and two individual transformations.

For both large scale purifications and small scale expression cultures, a single starter culture was used to inoculate all tested induction methods during each trial so that each set of induced cultures represented a set of monoclonal cultures.

3. Results

3.1. Low-level expression of Gal-3 CRD with IPTG

To produce the *Homo sapiens* Galectin-3 carbohydrate recognition domain (Gal-3 CRD, residues 112–250) to study its interactions with carbohydrates and carbohydrate-functionalized dendrimers [23,34,35], we first expressed a minimally, non-cleavable His₆-tagged construct using traditional IPTG induction. Gal-3 CRD was then purified using immobilized metal affinity chromatography (IMAC) and size exclusion chromatography. Following a previous protocol [36], induction with 0.1 mM IPTG gave 1.5 mg of purified Gal-3 CRD per gram of cell pellet. The purified fractions represented the majority of the Gal-3 CRD, as Gal-3 CRD in the pellet and flow through (FT) fractions appear minimal (Pellet and FT lanes, Fig. 2; Supplementary Table S3).

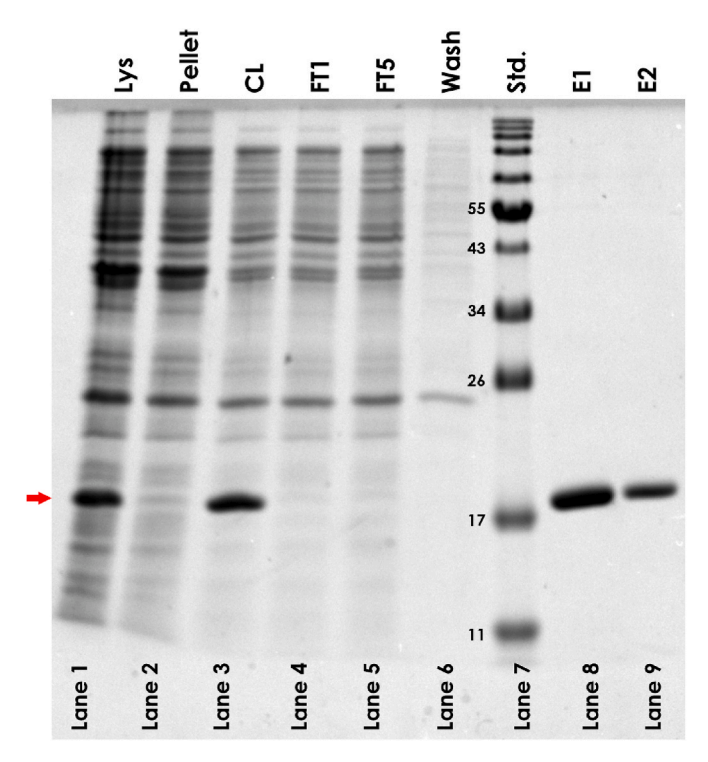


Fig. 2. Gal-3 CRD induction with 0.1 mM IPTG. The lysate (Lys, lane 1) shows a band at approximately 18 kDa (red arrow) consistent with Gal-3 CRD. Gal-3 CRD is also present in the cleared lysate (CL, lane 3), while flow-through fractions (FT1 and FT5, lanes 4 and 5) and the Wash fraction (Wash, lane 6) lack quantifiable Gal-3 CRD, signifying Gal-3 CRD is bound to the Ni-NTA resin. Elution fractions (E1 and E2, lanes 8 and 9) show relatively pure Gal-3 CRD.

To increase the expression levels of Gal-3 CRD, as suggested by Prato et al. [21], we then explored a range of IPTG concentrations, from 0.5 to 5.0 mM. Overall, 2 mM IPTG gave minimal effect, with yields of 1.35–1.79 mg protein/g cell pellet and increasing the IPTG concentration to 5 mM resulted in only a modest increase in Gal-3 CRD yield of 2.59 mg protein/g cell pellet.

Following this modest increase in Gal-3 CRD yields at these increased IPTG concentrations, we ran a series of small-scale expression experiments to assess an even wider range of IPTG concentrations (0–50 mM). We quantified the soluble Gal-3 CRD in the cleared lysate fraction and insoluble Gal-3 CRD in the resuspended lysate pellet fractions via SDS-PAGE (Supplementary Figs. S4 and S5). Peak Gal-3 CRD production from IPTG induction occurred at 10 mM IPTG, producing 16.2 mg of Gal-3 CRD per L of media, 25 % more than the 0.1 mM IPTG culture (Supplementary Table S4). Notably, further increases in IPTG concentrations did not increase overall yield but resulted in lower final OD $_{600}$ values, potentially due to the toxicity of this non-metabolizable lactose analog. Growth curves of nontransformed E. coli BL21 cells show slower growth and lower stationary phase densities as IPTG concentration increases.

3.2. Basal Gal-3 CRD expression in the absence of IPTG

In our attempts to increase expression levels with increased IPTG, the control culture lacking IPTG also produced 1.35 mg Gal-3 CRD/g cell pellet (Fig. 3). This suggested much of the Gal-3 CRD expressed in cultures containing ≤ 2 mM IPTG was a result of leaky expression rather than IPTG induction. Importantly, we also recognized that leaky expression of Gal-3 CRD could result in significant accumulation of Gal-3 CRD before the addition of IPTG. Further, because IPTG is a lactose analogue, we hypothesized that Gal-3 CRD produced by leaky expression might sequester cytosolic IPTG and block induction, resulting in

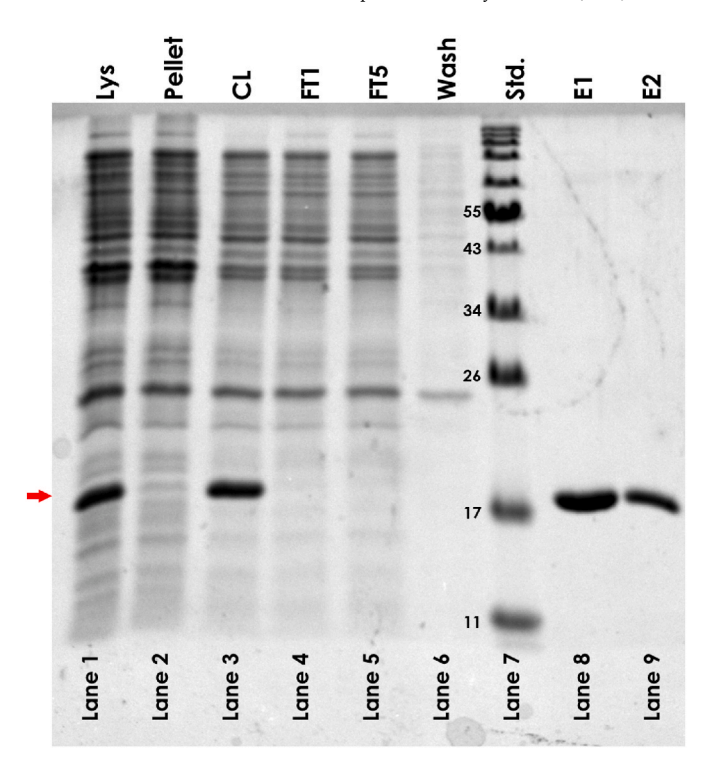
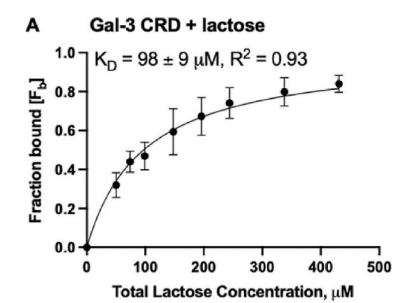


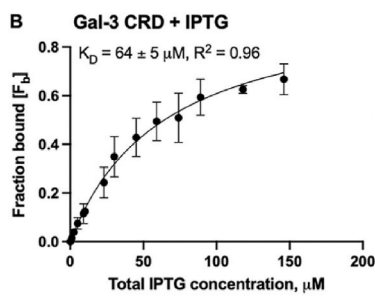
Fig. 3. Leaky expression of Gal-3 CRD. Control cultures grown without IPTG gave 1.35 mg of Gal-3 CRD per gram of cell pellet, nearly equivalent to IPTG-induced cultures. The red arrow (far left) indicates Gal-3 CRD (18 kDa), which is visible in the crude cell lysate (Lys, lane 1) and the cleared lysate (CL, lane 3). Flow-through fractions (FT1 and FT5, lanes 4 and 5) and wash fraction (Wash, lane 6) lack quantifiable Gal-3 CRD. Elution fractions (E1, E2, lanes 8 and 9) show relatively pure Gal-3 CRD.

feedback inhibition of Gal-3 CRD expression.

3.3. Gal-3 CRD binds IPTG

To address the hypothesis that Gal-3 CRD recognizes and sequesters IPTG, and to ensure Gal-3 CRD was properly folded and active for carbohydrate recognition, we measured the ability of Gal-3 CRD to bind both lactose and IPTG. Although many methods have been reported for studying the binding of carbohydrates by galectins [3], time-dependent fluorescence spectroscopy is a facile, highly accurate method for determining binding constants for lectin-carbohydrate interactions [23, 30]. As we previously reported, the fluorescence lifetime of Trp¹⁸¹, which is the only tryptophan present on Gal-3 CRD and is located directly in the glycoside binding site, can be used to follow ligand (e.g., lactose and IPTG) binding. The mean waveform at each ligand concentration is modeled as a linear combination of the carbohydrate-bound and free waveforms, yielding the fraction bound [23]. As shown in Fig. 4A and B, the time-resolved (sub-nanosecond) fluorescence emission waveforms yielded a K_D of 98 \pm 9 μM for Gal-3 CRD binding to lactose (Fig. 4A) and a K_D of 64 \pm 5 μM for the interaction between Gal-3 CRD and IPTG (Fig. 4B). Interestingly, the interaction between Gal-3 CRD and IPTG is slightly stronger than the affinity of the Gal-3 CRD for lactose. This is consistent with prior reports by Pieters and coworkers; the replacement of the anomeric oxygen with sulfur affords carbohydrate derivatives that are bound well by galectin CRDs [14,15]. Neither mannose nor glucose bind sufficiently to significantly alter the fluorescence lifetime of Trp¹⁸¹; these control experiments strongly suggest that IPTG and lactose are bound into the galectin CRD binding site (data are provided in the Supplementary Material). Similarly, the full-length galectin-3 binds IPTG with a K_D of 42 \pm 2 μM (Fig. 4C), which is also slightly higher affinity than our reported value





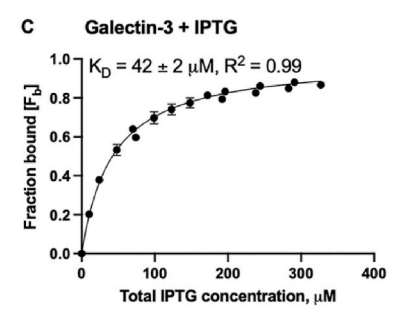


Fig. 4. Affinity of Galectin-3 for IPTG (A) Gal-3 CRD recognizes lactose with a K_D of $98\pm9~\mu M$ and (B) IPTG with slightly higher affinity, $64\pm5~\mu M$, while (C) full-length galectin-3 also recognizes IPTG with comparable affinity ($K_D=42\pm2~\mu M$). Each curve is the mean of at least 3 independent experiments using protein from two different Gal-3 CRD or full-length galectin-3 preparations. Error bars represent the standard deviation of the mean. The data were fit to the one-site single binding function in GraphPad Prism.

for lactose ($K_D=56\pm 8~\mu M$, also measured in a fluorescence lifetime binding experiment) [23]. When cell density, cell volume, and leaky expression levels of Gal-3 CRD in uninduced cultures are considered [37, 38], we calculate an intracellular Gal-3 CRD concentration of ~240 μM , well above the K_D (see "Cellular Concentration of Gal-3 CRD from Leaky Expression" in the Supplementary Data). Thus, the IPTG binding results support the hypothesis that galectin-3 binds and sequesters IPTG, in this case, damping induction and expression of Gal-3 CRD in a negative feedback loop.

3.4. Autoinduction produces high Gal-3 CRD yields

After identifying the potential for Gal-3 CRD to feedback inhibit its own induction with IPTG, we looked to autoinduction [24], a tool our lab has used extensively [26,39,40]. Similar to IPTG, autoinduction also utilizes the T7 expression system. However, rather than IPTG, autoinduction instead utilizes specific ratios of carbon sources, in this case glycerol, glucose, and lactose, to tune induction. Importantly, this also allowed us to utilize our existing vectors. We found that autoinduction reliably produced 10.8 mg \pm 1.0 mg Gal-3 CRD per gram of cell pellet (Fig. 5, Supplementary Data Tables S5 and S6), a more than 7-fold increase relative to 1 mM IPTG, and nearly 4 times more than 5.0 mM IPTG (Supplementary Data Table S6).

3.5. Autoinduction, expression, and purification of full-length Galectin-3

We also examined the effect of induction with various IPTG concentrations on full-length galectin-3. Like Gal-3 CRD, we found significant levels of leaky expression in noninduced cultures (0.5 mg/g cell pellet of cell pellet) and only a modest increase to 0.9 mg/g cell pellet when induced with up to 50 mM IPTG (Supplemental Fig. S6 and Supplemental Table S7). In contrast, when we utilized the autoinduction protocol developed for Gal-3 CRD, yields of full length galectin-3 rose to 2.5 mg/g cell pellet, or 25 mg per liter of media (Fig. 6). Thus, like Gal-3 CRD, autoinduction results in increased expression levels, giving a 5-fold increase per gram of cell pellet compared to the 0.1 mM IPTG culture, and an 8-fold increase with respect to culture volume.

4. Discussion

4.1. Comparison of autoinduction and IPTG-induced induction for galectin expressions

In classic work, Jacques Monod demonstrated diauxic growth in mixtures of glucose and lactose, where glucose, as the preferred carbon source, is metabolized first [41,42]. Glucose also inhibits uptake and catabolism of glycerol [43]. In this light, the Studier autoinduction protocol utilizes N-Z amine (amino acids), yeast extract and a mixture of glucose (0.05 %), lactose (0.2 %) and glycerol 0.5 %) [24]. When

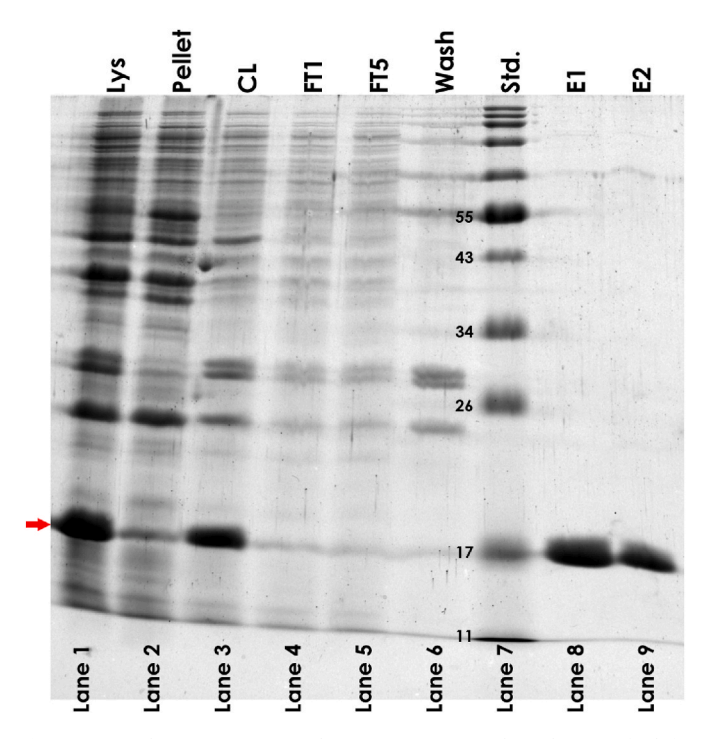


Fig. 5. Autoinduction increases Gal-3 CRD expression. The red arrow (far left) indicates Gal-3 CRD (18 kDa), which is visible in the crude cell lysate (Lys, lane 1) and the cleared lysate (CL, lane 3). Flow-through fractions (FT1 and FT5) and wash fraction (Wash) are shown in lanes 4–6, respectively. Elution fractions (E1, E2, lanes 8 and 9) show relatively pure Gal-3 CRD.

cultures are first inoculated in the presence of 0.05 % glucose, the uptake of lactose and glycerol are inhibited. However, as glucose and amino acids are exhausted, cAMP levels rise and engage the catabolite activator protein (CAP) [44]. Carbon catabolite repression is thus relieved (CCR, reviewed in Ref. [42]), and lactose and glycerol are then co-metabolized [24,43]. Importantly, in *E. coli* strains harboring prophage lambda DE3, the increased lactose levels drive expression of T7 RNA polymerase, which is under control of the lacUV5 promoter ($P_{la-cUV5}$) [45,46]. T7 RNA polymerase, in-turn, drives high-level transcription of a target gene under control of the T7 promoter, resulting in robust overexpression of the gene of interest [45,46].

With traditional IPTG induction protocols using LB media, IPTG concentrations are low (\sim 1 mM), and thus potentially susceptible to sequestration by cellular galectin resulting from leaky expression (Fig. 7), a well-established phenomenon in T7 expression systems [47]. In contrast, with autoinduction media, lactose concentrations are significantly higher (0.2 %, 6 mM), and though lactose concentrations

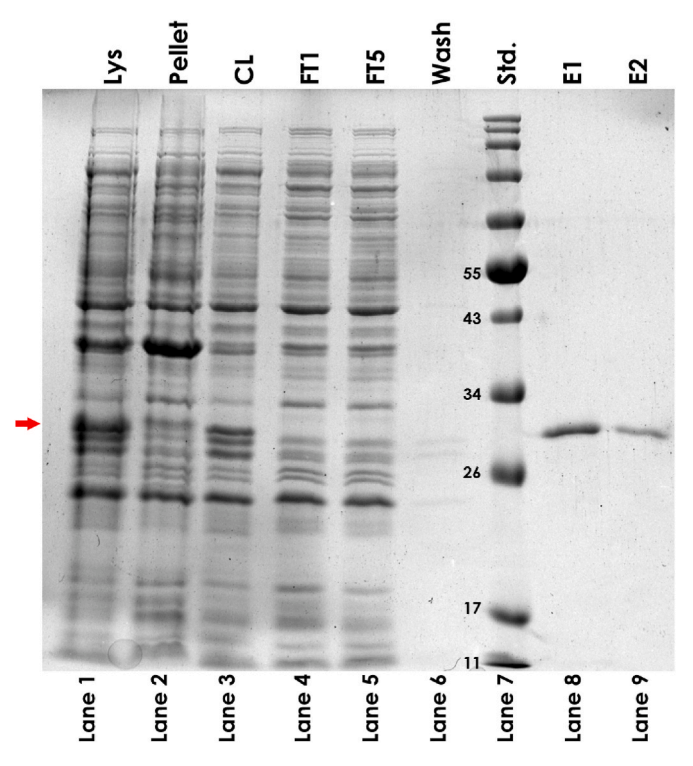


Fig. 6. Autoinduction efficiently produces full-length Galectin-3. The red arrow (far left) indicates galectin-3 (Gal-3, 26 kDa), which is visible in the crude cell lysate (Lys, lane 1) and the cleared lysate (CL, lane 3). Flow-through fractions (FT1 and FT5) and wash fraction (Wash) are shown in lanes 4–6, respectively. Elution fractions (E1, E2, lanes 8 and 9) show relatively pure galectin-3.

begin to fall as glucose is exhausted, this happens relatively slowly due to the presence of 54 mM glycerol as the major carbon source [24]. For this reason, free intracellular lactose is sustained, providing the requisite levels of T7 RNA polymerase needed for high level transcription.

Autoinduction media (ZYP-5052)) is a rich media, and from this point of view, is expected to provide increased cell mass, and thus greater yields in terms of mg of protein per liter of culture [24]. In our work, IPTG-induced LB media produced $5.0~g\pm0.3~g$ of cells per liter of media, whereas cell pellets derived from autoinduction were $9.5~g\pm0.2~g/L$, roughly a two-fold difference. It is for this reason that we have instead characterized the increased yield with respect to 1~g of cell pellet. As shown in Fig. 8, comparing mg of Gal-3 CRD purified from a gram of cell pellet (blue bars in Fig. 8), autoinduction increased yields by 7-fold compared to IPTG. Nevertheless, when yields are standardized to culture volume (orange bars in Fig. 8), the efficiency of autoinduction increases to $\sim\!14$ -fold higher than IPTG-induction. Similarly, autoinduction of full-length galectin-3 resulted in yields per liter of media $\sim\!5$ -fold higher than yields achieved using IPTG induction.

Many studies report the use of sub-millimolar concentrations of IPTG (75 μ M [18], 100 μ M [19,20,48], 400 μ M [49,50], and 500 μ M [51,52]) to induce expression of galectin-3 and/or Gal-3 CRD. However, some authors note that higher concentrations of IPTG (e.g., 1 mM) do afford higher yields of galectin-3 and Gal-3 CRD [21,53]. Although yields of galectin-3 are often not specified in published protocols, when yields of galectin-3 are reported, they are generally low. Raz and co-workers indicate expected yields of 1–5 mg of full-length galectin-3 per L culture (100 μ M IPTG, GST-tag) [48], which is very comparable to our yield of 3 mg at the same concentration of IPTG (Table S7). Likewise, Prato et al. note that the expected yield of galectins obtained using their protocol is "above 4 mg of protein" (1 mM IPTG) [21]. Using the autoinduction protocol provided herein, we obtain 25 mg of full-length galectin-3 per liter of cell culture, significantly higher than previously reported yields. Similarly, the autoinduction protocol reported herein

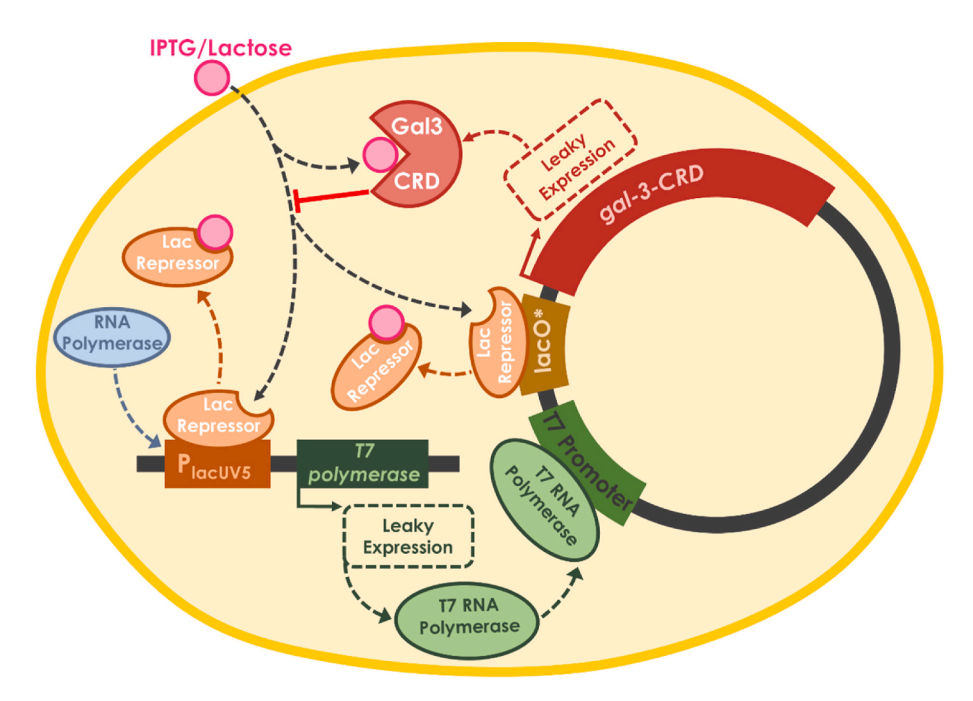


Fig. 7. Feedback inhibition. *E. coli* BL21 (DE3) carries a chromosomal copy of T7 RNA polymerase under control of the P_{lacUV5} promoter, such that expression of T7 RNA polymerase is inhibited by lac repressor (LacI). Upon addition of IPTG, transcriptional repression is relieved, driving expression of T7 RNA polymerase, which then binds the T7 promoter in various expression plasmids, inducing expression of the target gene. When the target gene is Gal-3 CRD or full-length galectin-3 (not shown), accumulating galectin levels may in-turn bind and sequester intracellular IPTG. Gal-3 CRD potentially outcompetes and deprives lac repressor of IPTG, resulting in repression of both the T7 RNA polymerase and $gal-3 \ crd$ genes. Gal-3 CRD and full-length galectin-3 may thus feedback inhibits its own production. Even in the absence of IPTG, low level expression of T7 RNA polymerase from the P_{lacUV5} promoter generally occurs, which may drive leaky expression of the target gene [24]. This is especially true in vectors like pDEST14 that lack secondary induction control, such as the lac operator (*). In the cases of Gal-3 CRD and full-length galectin-3, leaky expression levels appear to be high enough to sequester intracellular IPTG, inhibiting further production of the desired proteins.

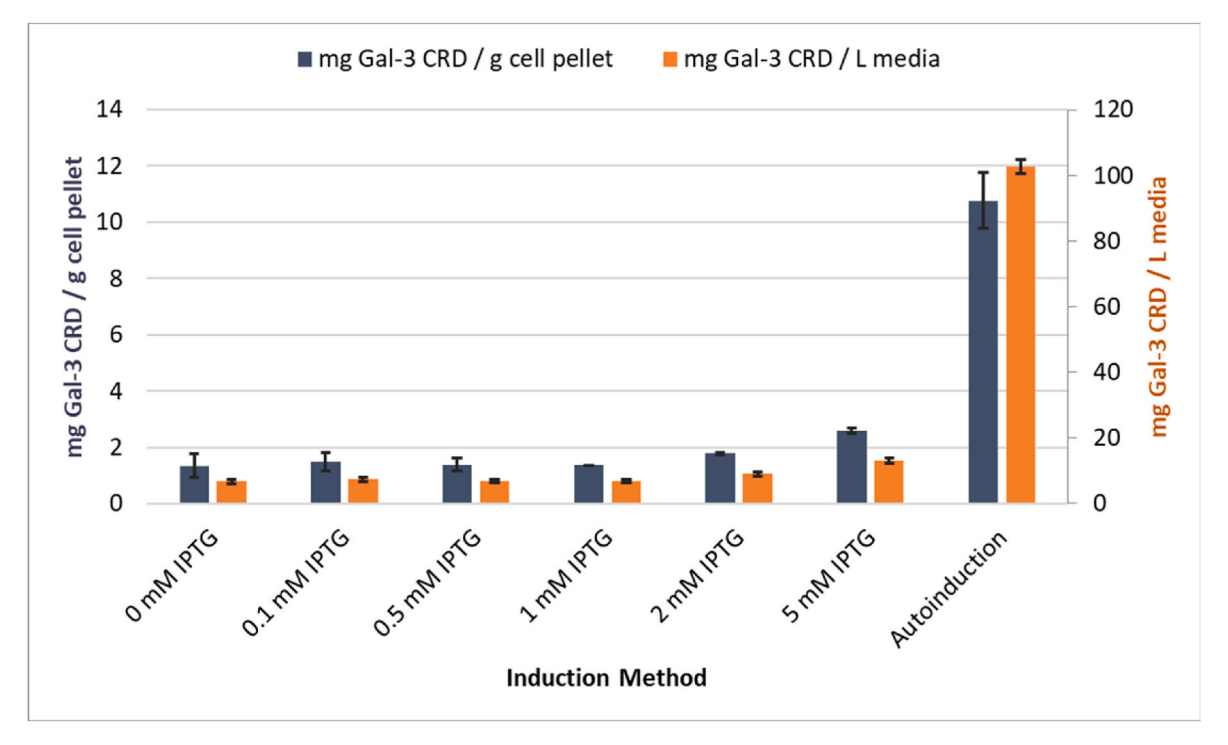


Fig. 8. Autoinduction outperforms IPTG. Autoinduction results in greater yields than IPTG induction, in terms of both mg protein/g cell pellet (blue bars) and mg protein/L of culture (orange bars). We consistently purified about 7 times more Gal-3 CRD per gram of cell pellet using autoinduction compared to induction with 0.1–1 mM IPTG. Mean yields and standard deviations represent three separate purifications for each induction method.

for Gal-3 CRD affords 100 mg/L of culture, which is 2 to 4-fold higher than the highest published yields [49,50] from IPTG induction protocols. Moreover, because the protein expression levels are higher, it is easier to fully load the IMAC resin with Gal-3 CRD, reducing levels of copurifying proteins from *E. coli*. Indeed, the material obtained after IMAC purification is sufficiently pure that additional chromatography is unnecessary. Lastly, because autoinduction eliminates the need for monitoring optical density prior to adding IPTG, autoinduction is a facile method for protein expression, one that worked extremely well for introductory-level researchers within the context of our course based undergraduate research experience.

5. Conclusion

The autoinduction protocol described here was used to produce ${\rm His}_{6}$ -tagged Gal-3 CRD and full-length galectin-3. with high yields and purities. The protocol also eliminates the need to monitor E. coli growth. Time-dependent fluorescence shows that galectin-3 and the Gal-3 CRD efficiently bind IPTG. Galectin-3 and its truncated variant can thus feedback inhibit their own expression when IPTG is used. Autoinduction overcomes this barrier to high level galectin-3 expression.

CRediT authorship contribution statement

Alexander A. Charbonneau: Writing – review & editing, Writing – original draft, Visualization, Validation, Methodology, Investigation, Formal analysis, Data curation, Conceptualization. Elizabeth J. Reicks: Investigation. John F. Cambria: Investigation. Jacob Inman: Investigation. Daria Danley: Investigation. Emmie A. Shockley: Investigation, Formal analysis. Ravenor Davion: Investigation, Formal analysis. Isabella Salgado: Investigation. Erienne G. Norton: Investigation. Lucy J. Corbett: Investigation. Lucy E. Hanacek: Investigation. Jordan G. Jensen: Investigation, Formal analysis. Marguerite A. Kibodeaux: Investigation. Tess K. Kirkpatrick: Investigation. Keilen M. Rausch: Investigation. Samantha R. Roth: Investigation, Formal analysis. Bernadette West: Investigation. Kenai E. Wilson: Investigation. C. Martin

Lawrence: Writing – review & editing, Writing – original draft, Resources, Project administration, Methodology, Funding acquisition, Conceptualization. Mary J. Cloninger: Writing – review & editing, Writing – original draft, Resources, Project administration, Methodology, Investigation, Funding acquisition, Formal analysis, Data curation, Conceptualization.

Declaration of competing interest

The authors declare that they have no competing interests.

Data availability

Data will be made available on request.

Acknowledgements

This research was funded by NSF CHE 2227874.

Appendix A. Supplementary data

Supplementary data to this article can be found online at https://doi.org/10.1016/j.pep.2024.106516.

References

- K.V. Marino, A.J. Cagnoni, D.O. Croci, G.A. Rabinovich, Targeting galectin-driven regulatory circuits in cancer and fibrosis, Nat. Rev. Drug Discov. 22 (2023) 295–316.
- [2] P. Navarro, N. Martinez-Bosch, A.G. Blidner, G.A. Rabinovich, Impact of galectins in resistance to anticancer therapies. Clin. Cancer Res. 26 (2020) 6086–6101.
- [3] C.M. Arthur, M.D. Baruffi, R.D. Cummings, S.R. Stowell, Evolving mechanistic insights into galectin functions, in: S.R. Stowell, R.D. Cummings (Eds.), Galectins: Methods and Protocols, 2015, pp. 1–35.
 [4] M.F. Troncoso, M.T. Elola, A.G. Blidner, L. Sarrias, M.V. Espelt, G.A. Rabinovich,
- [4] M.F. Troncoso, M.T. Elola, A.G. Blidner, L. Sarrias, M.V. Espelt, G.A. Rabinovich, The universe of galectin-binding partners and their functions in health and disease, J. Biol. Chem. 299 (2023) 105400.

- [5] G.G. Caballero, H. Kaltner, T.J. Kutzner, A.K. Ludwig, J.C. Manning, S. Schmidt, F. Sinowatz, H.J. Gabius, How galectins have become multifunctional proteins, Histol. Histopathol. 35 (2020) 509-539.
- [6] S. Sciacchitano, L. Lavra, A. Morgante, A. Ulivieri, F. Magi, G.P. De Francesco, C. Bellotti, L.B. Salehi, A. Ricci, Galectin-3: one molecule for an alphabet of diseases, from A to Z, Int. J. Mol. Sci. 19 (2018) 379.
- J. Nio-Kobayashi, Histological mapping and subtype-specific functions of galectins in health and disease, Trends Glycosci. Glycotechnol. 30 (2018) SE89-SE96.
- [8] R.P.M. Dings, N. Kumar, S. Mikkelson, H.-J. Gabius, K.H. Mayo, Simulating cellular galectin networks by mixing galectins in vitro reveals synergistic activity, Biochem. Biophys. Rep. 28 (2021) 101116, 101116.
- [9] S.R. Stowell, R.D. Cummings, Galectins: Methods and Protocols, Springer Science, New York, 2015.
- [10] R.D. Cummings, F.T. Liu, Galectins, in: A. Varki, R.D. Cummings, J.D. Esko, H. H. Freeze, P. Stanley, C.R. Bertozzi, G.W. Hart, M.E. Etzler (Eds.), Essentials of Glycobiology, second ed., Cold Spring Harbor Laboratory Press, Cold Spring Harbor (NY), 2009.
- [11] H.J. Gabius, M. Cudic, T. Diercks, H. Kaltner, J. Kopitz, K.H. Mayo, P.V. Murphy, S. Oscarson, R. Roy, A. Schedlbauer, S. Toegel, A. Romero, What is the sugar code? Chembiochem 23 (2023) e202100327.
- [12] S. Di Lella, V. Sundblad, J.P. Cerliani, C.M. Guardia, D.A. Estrin, G.R. Vasta, G. A. Rabinovich, When galectins recognize glycans: from biochemistry to physiology and back again, Biochemistry 50 (2011) 7842-7857.
- [13] S.P. Bernhard, M.S. Fricke, R. Haag, M.J. Cloninger, Protein aggregation nucleated by functionalized dendritic polyglycerols, Polym. Chem. 11 (2020) 3849-3862.
- [14] H. van Hattum, H.M. Branderhorst, E.E. Moret, U.J. Nilsson, H. Leffler, R.J. Pieters, Tuning the preference of thiodigalactoside- and lactosamine-based ligands to galectin-3 over galectin-1, J. Med. Chem. 56 (2013) 1350-1354.
- [15] M. van Scherpenzee, E.E. Moret, L. Ballell, R.M.J. Liskamp, U.J. Nilsson, H. Leffler, R.J. Pieters, Synthesis and evaluation of new thiodigalactoside-based chemical robes to label galectin-3, Chembiochem 10 (2009) 1724-1733.
- [16] D. Giguère, S. Sato, C. St-Pierre, S. Sirois, R. Roy, Aryl O- and S-galactosides and lactosides as specific inhibitors of human galectins-1 and -3: role of electrostatic potential at O-3, Bioorg. Med. Chem. Lett. 16 (2006) 1668–1672.
- I. Cumpstey, S. Carlsson, H. Leffler, U.J. Nilsson, Synthesis of a phenyl thio-β-Dgalactopyranoside library from 1,5-difluoro-2,4-dinitrobenzene: discovery of efficient and selective monosaccharide inhibitors of galectin-7, Org. Biomol. Chem. 3 (2005) 1922-1932.
- [18] T.K. Dam, H.J. Gabius, S. Andre, H. Kaltner, M. Lensch, C.F. Brewer, Galectins bind to the multivalent glycoprotein asialofetuin with enhanced affinities and a gradient of decreasing binding constants, Biochemistry 44 (2005) 12564–12571.

 [19] P.A. Poland, C.L. Kinlough, R.P. Hughey, Cloning, expression, and purification of
- galectins for in vitro studies, Galectins: Methods Protoc. 1207 (2015) 37–49.
- [20] P.A. Poland, C.L. Kinlough, R.P. Hughey, Cloning, expression, and purification of galectins for in vitro studies, Methods Mol. Biol. 2442 (2022) 41–54.
- [21] C.A. Prato, J. Carabelli, V. Cattaneo, O. Campetella, M.V. Tribulatti, Purification of recombinant galectins expressed in bacteria, Star Protocols 1 (2020) 100204.
- [22] C. Dey, P. Palm, L. Elling, Characterization of galectin fusion proteins with
- glycoprotein affinity columns and binding assays, Molecules 28 (2023) 1054. [23] S.P. Bernhard, C.K. Goodman, E.G. Norton, D.G. Alme, C.M. Lawrence, M. J. Cloninger, Time-dependent fluorescence spectroscopy to quantify complex binding interactions, ACS Omega 5 (2020) 29017-29024.
- [24] F.W. Studier, Protein production by auto-induction in high-density shaking cultures, Protein Expr. Purif. 41 (2005) 207-234.
- [25] S.K. Menon, B.J. Eilers, M.J. Young, C.M. Lawrence, The crystal structure of D212 from sulfolobus spindle-shaped virus ragged hills reveals a new member of the PD-(D/E)XK nuclease superfamily, J. Virol. 84 (2010) 5890-5897.
- [26] N.G. Lintner, K.A. Frankel, S.E. Tsutakawa, D.L. Alsbury, V. Copié, M.J. Young, J. A. Tainer, C.M. Lawrence, The structure of the CRISPR-associated protein Csa3 provides insight into the regulation of the CRISPR/Cas system, J. Mol. Biol. 405 (2011) 939-955.
- [27] G. Bertani, Studies on lysogenesis I, J. Bacteriol. 62 (1951) 293–300.
- [28] M.M. Bradford, A rapid and sensitive method for the quantitation of microgram quantities of protein utilizing the principle of protein-dye binding, Anal. Biochem. 72 (1976) 248-254.
- [29] A.I. Nesvizhskii, A. Keller, E. Kolker, R. Aebersold, A statistical model for identifying proteins by tandem mass spectrometry, Anal. Chem. 75 (2003) 4646-4658

- [30] S. Brown, C.C. Gauvin, A.A. Charbonneau, N. Burman, C.M. Lawrence, Csx3 is a cyclic oligonucleotide phosphodiesterase associated with type III CRISPR-Cas that degrades the second messenger cA(4), J. Biol. Chem. 295 (2020) 14963-14972.
- [31] K.J. Petersen, K.C. Peterson, J.M. Muretta, S.E. Higgins, G.D. Gillispie, D. D. Thomas, Fluorescence lifetime plate reader: resolution and precision meet highthroughput, Rev. Sci. Instrum. 85 (2014) 113101.
- J.M. Muretta, A. Kyrychenko, A.S. Ladokhin, D.J. Kast, G.D. Gillispie, D.D. Thomas, High-performance time-resolved fluorescence by direct waveform recording, Rev. Sci. Instrum. 81 (2010) 103101.
- [33] K.H. Schlick, C.K. Lange, G.D. Gillispie, M.J. Cloninger, Characterization of protein aggregation via intrinsic fluorescence lifetime, J. Am. Chem. Soc. 131 (2009)
- [34] J.H. Ennist, H.R. Termuehlen, S.P. Bernhard, M.S. Fricke, M.J. Cloninger, Chemoenzymatic synthesis of galectin binding glycopolymers, Bioconjugate Chem. 29 (2018) 4030-4039.
- [35] C.K. Goodman, M.L. Wolfenden, P. Nangia-Makker, A.K. Michel, A. Raz, M. J. Cloninger, Multivalent scaffolds induce galectin-3 aggregation into nanoparticles, Beilstein J. Org. Chem. 10 (2014) 1570-1577.
- E.T. Larson, D. Reiter, M. Young, C.M. Lawrence, Structure of A197 from sulfolobus turreted icosahedral virus: a crenarchaeal viral glycosyltransferase exhibiting the GT-A fold, J. Virol. 80 (2006) 7636-7644.
- [37] H.E. Kubitschek, J.A. Friske, Determination of bacterial-cell volume with the Coulter-Counter, J. Bacteriol. 168 (1986) 1466-1467.
- [38] J.A. Myers, B.S. Curtis, W.R. Curtis, Improving accuracy of cell and chromophore concentration measurements using optical density, BMC Biophys. 6 (2013) 4.
- [39] S. Brown, C.C. Gauvin, A.A. Charbonneau, N. Burman, C.M. Lawrence, Csx3 is a cyclic oligonucleotide phosphodiesterase associated with type III CRISPR-Cas that degrades the second messenger cA4, J. Biol. Chem. 295 (2020) 14963-14972.
- [40] A.A. Charbonneau, D.M. Eckert, C.C. Gauvin, N.G. Lintner, C.M. Lawrence, Cyclic tetra-adenylate (cA4) recognition by Csa3; implications for an integrated class 1 CRISPR-cas immune response in saccharolobus solfataricus. Biomolecules 11 (2021) 1852.
- [41] J. Monod, The growth of bacterial cultures, Annu. Rev. Microbiol. 3 (1949) 371,
- J. Stulke, W. Hillen, Carbon catabolite repression in bacteria, Curr. Opin. [42] Microbiol. 2 (1999) 195-201.
- [43] K. Bettenbrock, S. Fischer, A. Kremling, K. Jahreis, T. Sauter, E.D. Gilles A quantitative approach to catabolite repression in Escherichia coli, J. Biol. Chem. 281 (2006) 2578–2584.
- [44] D. Voet, J.G. Voet, Biochemistry, John Wiley & Sons, Hoboken, NJ, 2011.
- [45] F.W. Studier, B.A. Moffatt, Use of bacteriophage T7 RNA polymerase to direct selective high-level expression of cloned genes, J. Mol. Biol. 189 (1986) 113-130.
- [46] F.W. Studier, A.H. Rosenberg, J.J. Dunn, J.W. Dubendorff, Use of T7 RNA polymerase to direct expression of cloned genes, Methods Enzymol. 185 (1990) 60-89.
- [47] L.C. Anthony, H. Suzuki, M. Filutowicz, Tightly regulated vectors for the cloning and expression of toxic genes, J. Microbiol. Methods 58 (2004) 243-250.
- P. Nangia-Makker, V. Balan, A. Raz, Galectin-3 binding and metastasis, in: M. Dwek, S.A. Brooks, U. Schumacher (Eds.), Metastasis Res. Protoc., Humana Press, Totowa, NJ, 2012, pp. 251-266.
- C. Diehl, S. Genheden, K. Modig, U. Ryde, M. Akke, Conformational entropy changes upon lactose binding to the carbohydrate recognition domain of galectin-3, J. Biomol, NMR 45 (2009) 157-169.
- [50] M.C. Miller, Y. Zheng, D. Suylen, H. Ippel, F.J. Canada, M.A. Berbis, J. Jimenez-Barbero, G. Tai, H.-J. Gabius, K.H. Mayo, Targeting the CRD F-face of human galectin-3 and allosterically modulating glycan binding by angiostatic PTX008 and a structurally optimized derivative, ChemMedChem 16 (2021) 713-723.
- [51] S.A. Farhadi, R.J. Liu, M.W. Becker, E.A. Phelps, G.A. Hudalla, Physical tuning of galectin-3 signaling, Proc. Natl. Acad. Sci. U.S.A. 118 (2021).
- H. Zhang, D. Laaf, L. Elling, R.J. Pieters, Thiodigalactoside-bovine serum albumin conjugates as high-potency inhibitors of galectin-3: an outstanding example of multivalent presentation of small molecule inhibitors, Bioconjugate Chem. 29 (2018) 1266-1275.
- [53] P.K. Vemuri, N.R. Varakala, D. Dhakate, T. Ravavarapu, F.P. Dumpala, S. S. Muddana, H. Bommepalli, S. Modiboyana, Improving the recombinant protein expression of human galectin-3 in BL21 bacterial host system, J. Pharm. Res. Int. 32 (2020) 111-115.